MOLECULAR AND CELLULAR BIOLOGY, Dec. 2010, p. 5698–5709 Vol. 30, No. 24
0270-7306/10/$12.00 doi:10.1128/MCB.00165-10

Oligomerization of the Mitochondrial Protein Voltage-Dependent Anion Channel Is Coupled to the Induction of Apoptosis[▽]

Nurit Keinan, Dalia Tyomkin, and Varda Shoshan-Barmatz*

Department of Life Sciences and National Institute for Biotechnology in the Negev, Ben-Gurion University of the Negev, Beer-Sheva, Israel

Received 10 February 2010/Returned for modification 11 April 2010/Accepted 27 September 2010

Accumulating evidence implicates that the voltage-dependent anion channel (VDAC) functions in mitochondrion-mediated apoptosis and as a critical player in the release of apoptogenic proteins, such as cytochrome *c*, triggering caspase activation and apoptosis. The mechanisms regulating cytochrome *c* release and the molecular architecture of the cytochrome *c*-conducting channel remain unknown. Here the relationship between VDAC oligomerization and the induction of apoptosis was examined. We demonstrated that apoptosis induction by various stimuli was accompanied by highly increased VDAC oligomerization, as revealed by cross-linking and directly monitored in living cells using bioluminescence resonance energy transfer technology. VDAC oligomerization was induced in all cell types and with all apoptosis inducers used, including staurosporine, curcumin, As_2O_3, etoposide, cisplatin, selenite, tumor necrosis factor alpha (TNF-α), H_2O_2, and UV irradiation, all acting through different mechanisms yet all involving mitochondria. Moreover, correlation between the levels of VDAC oligomerization and apoptosis was observed. Furthermore, the apoptosis inhibitor 4,4′-diisothiocyanostilbene-2,2′-disulfonic acid (DIDS) inhibited VDAC oligomerization. Finally, a caspase inhibitor had no effect on VDAC oligomerization and cytochrome *c* release. We propose that VDAC oligomerization is involved in mitochondrion-mediated apoptosis and may represent a general mechanism common to numerous apoptogens acting via different initiating cascades. Thus, targeting the oligomeric status of VDAC, and hence apoptosis, offers a therapeutic strategy for combating cancers and neurodegenerative diseases.

It is well accepted that mitochondria serve as integrators and amplifiers of programmed cell death through the regulation of apoptosis, mediating the release of proapoptotic proteins and/or disrupting cellular energy metabolism (25). During the transduction of an apoptotic signal into the cell, an alteration in mitochondrial membrane permeability occurs, facilitating the release of apoptogenic proteins, such as cytochrome *c* (Cyto *c*), apoptosis-inducing factor (AIF), and Smac/DIABLO, from the intermembrane space into the cytosol (45). These proteins participate in complex processes resulting in the activation of proteases and nucleases, leading to protein and DNA degradation and, ultimately, cell death (25). However, it remains unclear how these apoptotic initiators cross the outer mitochondrial membrane (OMM) and are released into the cytosol. While some models predict that such release is facilitated by swelling of the mitochondrial matrix and subsequent rupture of the OMM, other models predict the formation of protein-conducting channels that are large enough to allow the passage of Cyto *c* and other proteins into the cytosol without compromising OMM integrity (15, 44, 47). The voltage-dependent anion channel (VDAC) offers such a route (45).

Located in the OMM, the VDAC forms the main interface between the mitochondrial and cellular metabolisms by mediating the fluxes of ions, nucleotides, and other metabolites across the OMM (44). The topology and 3-dimensional (3D) structure of recombinant human and murine VDAC1 (hVDAC1 and mVDAC1) were recently solved by nuclear magnetic resonance (NMR) spectroscopy (12, 23) and X-ray crystallography (55), respectively. Such analyses revealed that VDAC1 adopts a β-barrel architecture composed of 19 β-strands, with an α-helix positioned horizontally, midway within the pore.

The VDAC has been proposed to function in mitochondrion-mediated apoptosis, based on several lines of experimental evidence. It has been shown that anti-VDAC antibodies inhibit Cyto *c* release, the interaction of Bax with the VDAC, and the triggering of cell death (29, 42, 65). The VDAC is, moreover, the proposed target of pro- and antiapoptotic members of the Bcl2 family (39, 42, 53) and of hexokinase I (HK-I) and HK-II (3, 7, 8, 41, 61). Furthermore, small interfering RNA (siRNA)-mediated downregulation of VDAC1 expression prevented cisplatin-induced Bax activation; strongly reduced the cisplatin-induced release of Cyto *c* and AIF, as well as the maturation of caspase-3 (51); and attenuated endostatin-induced apoptosis (60). Finally, overexpression of human, murine, yeast, and rice VDAC1 was found to induce apoptotic cell death, regardless of the cell type used (3, 19, 61), while arbutin (hydroquinone-*O*-β-D-glucopyranoside) induced apoptosis by inducing VDAC1 overexpression (35). On the other hand, VDAC proteins have been reported to be dispensable for Ca^{2+}- and oxidative-stress-induced permeability transition pore (PTP) opening (10). It has been suggested that multiple pathways and mechanisms of Cyto *c* release can coexist within a single model of cell death, depending on the cell type and the nature of the stimuli (18–20).

Despite this body of work pointing to the VDAC as a key player in apoptosis, major questions remain unanswered, such as the molecular architecture of the Cyto *c*-conducting chan-

* Corresponding author. Mailing address: Department of Life Sciences, Ben-Gurion University of the Negev, P.O. Box 653, Beer-Sheva 84105, Israel. Phone: 972-8-6461336. Fax: 972-8-6479207. E-mail: vardasb@bgu.ac.il.

▽ Published ahead of print on 11 November 2010.

nel. The channel pore resembles a slightly elliptical cylinder with horizontal dimensions of approximately 3.1 by 3.5 nm and a height of approximately 4 nm (12); NMR studies have indicated a diameter of about 2.5 nm for the open state (23), while the X-ray-based structure suggested maximal inner dimensions of 2.7 by 2.4 nm (55). Similar dimensions were also obtained from high-resolution atomic force microscopy (AFM) (height, 3.8 nm; diameter, 2.7 nm) (21) and electron microscopy (EM) (diameter, ~3 nm) (22) studies for VDAC proteins in the native state derived from *Saccharomyces cerevisiae* in its natural membrane composition. This pore size is large enough for the movement of nucleotides and small molecules but too small to allow the passage of a folded protein, such as Cyto *c* (diameter, 3.4 nm). One possible solution for this apparent paradox places the protein-conducting channel within a VDAC1 homo-oligomer or in a hetero-oligomer containing VDAC1 and proapoptotic proteins (1, 44, 47). Substantial evidence for the formation of higher-order VDAC-containing complexes exists. On the basis of EM of the 2D crystallized outer membrane, it was noted that VDAC pores are organized in ordered arrays, each bearing six monomers with interchannel contacts (22). VDACs from various sources have been shown to assemble into dimers, trimers, tetramers, and higher oligomeric states in a dynamic process, including the VDAC purified from liver mitochondria (62), recombinant human VDAC (63), and liver (62) or brain (48) mitochondrion-embedded VDAC. The supramolecular organization of the VDAC has also been demonstrated using AFM (21, 24). In addition, the use of symmetry operators on the NMR-based structure of recombinant hVDAC1 implied that it forms a dimer of monomers arranged in parallel (12). Furthermore, recent analysis of the crystal packing of mVDAC1 revealed strong antiparallel dimers that further assemble as hexamers (54).

The function of VDAC oligomers, however, remains to be proven. To address our hypothesis that oligomeric VDAC1 mediates the release of Cyto *c*, we investigated the relationship between VDAC oligomerization, Cyto *c* release, and cell death in this study. We found that apoptotic cell death induced by various stimuli, including chemotherapy agents, overexpression of VDAC1, UV irradiation, and H_2O_2, was accompanied by an increase as high as 20-fold in VDAC oligomerization. Moreover, apoptosis inhibitors also prevented VDAC oligomerization. We further explored the relationship between the oligomeric state of VDAC and apoptosis by using the BRET2 (bioluminescence resonance energy transfer) (4) approach, which allows direct monitoring of VDAC oligomerization in living cells. Our results indicate that VDAC1 oligomerization is associated with Cyto *c* release and apoptosis induction.

MATERIALS AND METHODS

Materials. Arsenic(III) oxide (As_2O_3), etoposide, 4,4′-diisothiocyanostilbene-2,2′-disulfonic acid (DIDS), poly-D-lysine (PDL), propidium iodide (PI), curcumin, sodium selenite, and staurosporine (STS) were purchased from Sigma (St. Louis, MO). Cisplatin was obtained from Fluka Biochemika. Ethylene glycol-bis(succinimidylsuccinate) (EGS) was obtained from Pierce. Human tumor necrosis factor alpha (TNF-α) was obtained from Cytolab (Rehovot, Israel). H_2O_2 was obtained from Acros Organics (Fair Lawn, NJ). Metafectene was purchased from Biontex (Munich, Germany). The MitoTracker Red dye CMXRos was obtained from Molecular Probes. The growth medium, Dulbecco's modified Eagle medium (DMEM), and the supplements, fetal calf serum, L-glutamine, and penicillin-streptomycin, were purchased from Biological Industries (Beit Haemek, Israel). Blasticidin was purchased from InvivoGen (San Diego, CA). Coelenterazine (DeepBlueC [DBC]) was obtained from Bioline (Taunton, MA). Monoclonal anti-VDAC antibodies directed against the N-terminal region of human porin 31HL came from Calbiochem-Novobiochem (Nottingham, United Kingdom). Monoclonal anti-actin and polyclonal anti-Bak antibodies were obtained from Santa Cruz Biotechnology (Santa Cruz, CA). Monoclonal anti-Cyto *c* antibodies were obtained from BD Biosciences Pharmingen (San Jose, CA). Polyclonal anti-Bid antibodies were obtained from R&D Systems (Minneapolis, MN). Monoclonal anti-Bax antibodies were obtained from Trevigen (Gaithersburg, Maryland). Horseradish peroxidase (HRP)-conjugated anti-mouse antibodies were obtained from Promega (Madison, WI). The pancaspase inhibitor benzyloxycarbonyl-Val-Ala-Asp(OMe)-fluoromethylketone (z-VAD-fmk) was obtained from Enzo Life Sciences AG (Lausen, Switzerland).

Plasmids. DNA encoding mVDAC1 (obtained from W. J. Craigen, University of Houston) or mutated E72Q-mVDAC1 or E202Q-mVDAC1 was cloned into the pcDNA4/TO vector to allow for tetracycline-regulated expression, as described previously (3). Rat muscle VDAC1 cDNA was cloned into the pcDNA4/TO vector and sequenced.

(i) Plasmids encoding fusion proteins. Plasmids encoding the fusion proteins rVDAC1-GFP2 and rVDAC1-Luc were constructed using BRET2 plasmids (Perkin-Elmer, Waltham, MA), and both luciferase and a variant of green fluorescent protein (GFP2) were fused to the C-terminal part of the protein. The rat VDAC1 (rVDAC1) gene was cloned into the BamHI and HindIII sites of the BRET2 plasmids (N2 variants). The rVDAC1 gene was amplified using forward primer CGAAGCTTATGGCTGTGCCACCCACGTATGCC and reverse primer GGATCCGCCGCCGCCGGAGCCGCCGCCGCCTGC TTGAAATTC. The reverse primer was designed to contain a double linker sequence. The double linker [$(GGGGS)_2$] connecting the VDAC1 and *RLuc* or *GFP2* genes allows the flexibility of the region (the linker sequence includes four glycines and one serine [9]).

(ii) Plasmids carrying shRNA against hVDAC1. Specific silencing of endogenous human VDAC1 (hVDAC1) was achieved using a vector expressing short hairpin RNA (shRNA). The sequence carrying the hVDAC1 shRNA was created using the following two complementary oligonucleotides, each containing the 19-nucleotide target sequence of hVDAC1 (nucleotides 337 to 355), followed by a short spacer and an antisense sequence of the target: oligonucleotide 1 (AGCTTAAAAACACTAGGCACCGAGATTATCTCTTGAATAATCTCGG TGCCTAGTGG) and oligonucleotide 2 (GATCCACACTAGGCACCGAGAT TATTCAAGAGATAATCTCGGTGCCTAGTGTTTTTTA). The sequence carrying the hVDAC1 shRNA was cloned into the BglII and HindIII sites of the pSUPERretro plasmid (OligoEngine, Seattle, WA), containing a puromycin resistance gene. Transcription of this sequence under the control of the H1 RNA polymerase III promoter produces a hairpin (hVDAC1 shRNA).

Tissue culture. T-REx-293 cells (HEK cells stably containing the pcDNA6/TR regulatory vector and thus expressing the tetracycline repressor) (Invitrogen) and T-REx-293 cells stably expressing hVDAC1 shRNA, showing low (10 to 20%) endogenous VDAC1 expression (referred to as T-REx-pS10 cells), were grown at 37°C under an atmosphere of 95% air and 5% CO_2 in DMEM supplemented with 10% fetal calf serum, 2 mM L-glutamine, 1,000 U/ml penicillin, 1 mg/ml streptomycin, and 5 μg/ml blasticidin. The HeLa and T47D cell lines were grown under the same conditions as T-REx-293 cells, except that blasticidin was not added. For T47D cells, insulin (20 U/ml) and 10 mM HEPES (pH 7.3) were added.

Cell transfection. T-REx-293 cells at ~50% confluence were transiently transfected (using Metafectene) with plasmid pcDNA4/TO encoding either rVDAC1 or native or mutated mVDAC1. Protein expression was induced by tetracycline (2.5 μg/ml) for 72 to 110 h before the cells were subjected to apoptosis induction and cross-linking analysis. In the BRET2 experiments, T-REx-pS10 cells were transfected using the calcium phosphate method. Transfections were carried out with 0.1 μg of a plasmid coding for rVDAC1–Rluc (*Renilla* luciferase [RLuc] fused to the VDAC1 C terminus) and with 0.8 μg of a plasmid coding for rVDAC1–GFP2 (GFP2 fused to the VDAC1 C terminus). Cells were analyzed for apoptosis induction and were subjected to the BRET2 assay 48 to 72 h posttransfection. As a negative control, cells were transfected with plasmids encoding rVDAC1–Rluc (0.1 μg) and GFP2 (0.8 μg). As another control (control cells), cells were transfected with plasmids encoding rVDAC1–Rluc (0.1 μg) and with plasmid pcDNA4/TO (0.8 μg).

BRET2 assay. For the BRET2 assay, we first established the appropriate conditions for resolving VDAC1 oligomerization using BRET2 technology in mammalian living cells. These included the number of cells to be plated, the amounts and ratios of the rVDAC1–Rluc and rVDAC1–GFP2 plasmids, the

apoptosis inducer concentration, the time of incubation, and the concentration of the luciferase substrate DBC. Cells transiently expressing rVDAC1–Rluc and rVDAC1–GFP2, as well as control cells, were incubated with the apoptosis inducer. Following incubation, cells were harvested, washed twice with phosphate-buffered saline (PBS), resuspended in 200 μl of PBS, and divided between 2 wells of a 96-well clear-bottom plate (Grenier). Luciferase activity was assayed using the membrane-permeant substrate DBC in PBS supplemented with $MgCl_2$ (1 g/liter) and glucose (1 g/liter), with DBC added to a final concentration of 5 μM just before luminescence measurements.

The BRET2 signal represents the ratio of the GFP2 fluorescence, measured at its emission wavelength (510 nm), to the light intensity (luminescence) emitted at 395 nm. All measurements were performed using the Infinite 200 ELISA reader (Tecan). BRET2 signals were defined as the GFP2/RLuc intensity ratio, which was calculated as follows. (i) The BRET2 signals obtained with VDAC1–Rluc/pcDNA4/TO cells (control cells) were subtracted from the signals obtained with cells expressing VDAC1–Rluc and VDAC1–GFP2–BRET2. (ii) The net ratios of RLuc and GFP2 activities (the GFP2/luciferase ratio after the subtraction of the BRET2 signals obtained from control cells) were calculated. (iii) The ratios of BRET2 signals between cells that were and were not exposed to apoptosis inducers were compared.

Apoptotic cell analysis. Staining with acridine orange (AcrOr) and ethidium bromide (EthBro) was carried out to analyze the extent of apoptosis (early and late apoptotic cells), as described previously (61). Stained cells were visualized by fluorescence microscopy (Olympus IX51 microscope), and images were recorded with an Olympus DP70 camera, using a superwide band filter. In each independent experiment in which early and late apoptotic cells were considered, approximately 300 cells were counted for each treatment. T-REx-293 or HeLa cells (2×10^6 to 4×10^6) treated with PI and annexin V–fluorescein isothiocyanate (FITC) were exposed to UV irradiation or other treatments, collected (at $1,500 \times g$ for 5 min), washed, and resuspended in 400 μl binding buffer (10 mM HEPES-NaOH [pH 7.4], 140 mM NaCl, and 2.5 mM $CaCl_2$). Annexin V–FITC was added to a final concentration of 4.5 μg/ml, and the cells were incubated in the dark for 15 min. Cells were then washed twice with binding buffer and were resuspended in 400 μl binding buffer, to which PI was added immediately before fluorescence-activated cell sorter (FACS) analysis. At least 10,000 events were recorded, represented as dot plots, and analyzed by software designed for use with the FACSCalibur flow cytometer (BD Biosciences, Franklin Lakes, NJ).

Cyto *c* release. Cells (5×10^4) were grown on PDL-coated coverslips in a 60-mm-diameter plate. After 24 h, cells were treated with selenite (8 μM; 17 h), followed by staining with MitoTracker Red dye (25 nM) for 15 min (37°C; 5% CO_2). PBS-washed cells were then fixed with 4% paraformaldehyde for 15 min, immunostained using anti-Cyto *c* antibodies and Alexa Fluor 488-conjugated secondary antibodies, and visualized by confocal microscopy (Olympus 1X81 microscope).

Cross-linking experiments. T-Rex-293, HeLa, or T47D cells (2.2 to 3 mg/ml in PBS [pH 8.2]) were harvested after the appropriate treatment and were incubated with cross-linking reagents (either EGS for 15 min or 1,5-difluoro-2,4-dinitrobenzene [DFDNB] for 30 min) at 30°C. Samples (60 to 100 μg) were subjected to sodium dodecyl sulfate-polyacrylamide gel electrophoresis (SDS-PAGE) and immunoblotting using anti-VDAC antibodies. Quantitative analysis of immunoreactive VDAC dimer and trimer bands was performed using Image Gauge (version 4.0; Science Lab 2001) software provided by the manufacturer (Fujifilm).

Caspase activation and activity assays. The activities of caspases 3 and 7 (caspase-3/7) in HeLa cells were assayed by using the ApoLive-Glo multiplex assay kit (Promega, Madison, WI) as described in the manufacturer's protocol. Briefly, the enzymatic activity of caspase-3/7 was measured by the caspase cleavage of a luminogenic caspase-3/7 substrate containing the tetrapeptide sequence DEVD, followed by the generation of a luminescent signal produced by luciferase. The bioluminescent signal was measured using a microplate reader. In addition, caspase activation was visualized by immunoblot analysis for cleavage of poly(ADP-ribose) polymerase (PARP) using a rabbit anti-PARP polyclonal antibody (Cell Signaling, Danvers, MA) and an HRP-conjugated goat anti-rabbit IgG antibody, followed by a chemiluminescence detection system (EZ-ECL kit; Biological Industries, Kibbutz Beit Haemek, Israel).

Gel electrophoresis and immunoblot analyses. Following SDS-PAGE, gels were either stained with Coomassie blue or immunoblotted with monoclonal anti-VDAC antibodies, followed by incubation with HRP-conjugated anti-mouse IgG secondary antibodies. Antibody labeling was detected by chemiluminescence. Prior to immunoblotting, membranes were treated with 0.1 M glycine (pH 2.0) and washed several times with Tris-Saline buffer.

RESULTS

Apoptosis induction by various stimuli induces VDAC oligomerization. In a previous study of isolated mitochondria (62), we showed, with several chemical cross-linking reagents, that VDAC assumes oligomeric states. In this study, we analyzed the oligomeric status of VDAC in cultured cells under physiological and apoptotic conditions. To obtain information on the oligomeric state of VDAC under apoptotic conditions, cells were first exposed to an apoptosis inducer and then incubated with the membrane-permeant cross-linker EGS. VDAC oligomeric states were then examined by SDS-PAGE and Western blotting using anti-VDAC antibodies.

The abilities of various apoptosis-inducing agents, acting via different mechanisms, to induce VDAC oligomerization in cultured cells are shown in Fig. 1. When T-REx-293 cells were challenged with staurosporine (STS), curcumin, tumor necrosis factor alpha (TNF-α), etoposide, cisplatin, or As_2O_3, all these agents induced VDAC oligomerization, as revealed by EGS-based cross-linking and immunoblotting using anti-VDAC antibodies (Fig. 1A). Several distinct (68-, 99-, and 136-kDa) anti-VDAC1 antibody-labeled protein bands, the same as those observed in isolated mitochondria, were clearly seen (Fig. 1) and were found to correspond to homodimers, trimers, and tetramers of the VDAC (62), as well as to high-molecular-weight complexes containing the VDAC. VDAC oligomerization was dramatically increased (as much as 20-fold) upon exposure to all apoptosis stimuli tested (Fig. 1A), suggesting that upon apoptosis induction, the dynamic equilibrium between monomeric and oligomeric forms of the VDAC was shifted toward the formation of dimers, trimers, tetramers, and multimers. As expected, treatment of the cells with the apoptosis-inducing agents listed above resulted in apoptotic cell death (Fig. 1A, bottom). Interestingly, an anti-VDAC1 antibody-labeled protein band migrating below the position of monomeric VDAC was obtained upon apoptosis induction and EGS treatment (arrows in Fig. 1B, 6A, and 7C). This band most likely represents a monomer that experienced intermolecular cross-linking that modified its mobility. This band appeared only when apoptosis was induced, suggesting that upon apoptosis induction, the VDAC underwent conformational changes that were fixed by EGS.

Sodium selenite, previously shown to induce oxidative stress, permeability transition pore opening (40), and apoptosis (52), also induced VDAC oligomerization (Fig. 1B). Immunofluorescence analysis of Cyto *c* release, carried out by confocal microscopy using anti-Cyto *c* antibodies, indicated that most cells released Cyto *c* in response to treatment with 8 μM selenite (Fig. 1C). This suggests that cell death triggered by selenite eventually converges toward VDAC oligomerization and "canonical apoptotic execution." In addition to chemotherapy reagents, exposure to UV irradiation or H_2O_2 resulted in VDAC oligomerization. The levels of VDAC dimers, trimers, and multimers increased upon H_2O_2 treatment (Fig. 2A) or with increasing time of UV irradiation (Fig. 2C). The induction of apoptotic cell death under the same conditions used to induce VDAC oligomerization was clearly observed upon cell death analysis by FACS-based quantification of annexin V–FITC–propidium iodide (PI) fluorescence (Fig. 2D) or PI uptake (Fig. 2B).

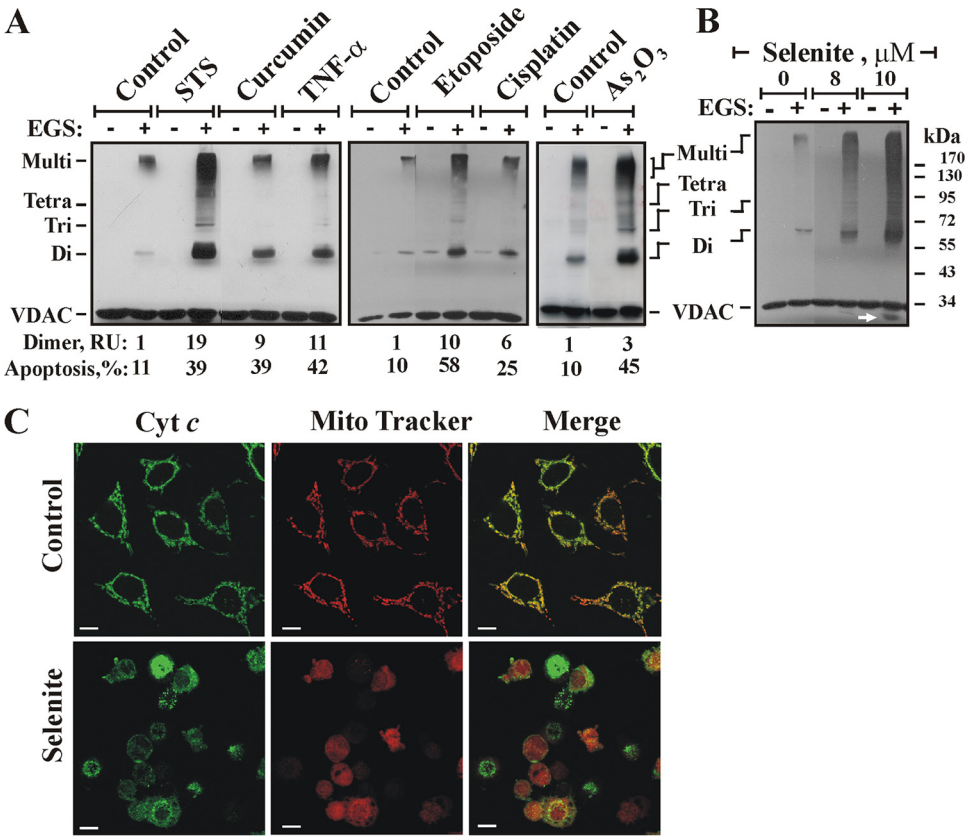

FIG. 1. Apoptosis induction is associated with VDAC oligomerization. (A) Cells were exposed either to STS (1.25 μM) for 2.5 h or to curcumin (40 μM), TNF-α (12 ng/ml), etoposide (2 μM), cisplatin (40 μM), or As_2O_3 (30 μM) for 16 h. Cells washed with PBS at 2.5 to 3 mg/ml were incubated with EGS (250 to 300 μM) at 30°C for 15 min and were then subjected to SDS-PAGE and immunoblotting using anti-VDAC antibodies. The positions of VDAC monomers to multimers are indicated. Percentages of apoptotic cells (assayed via AcrOr-EthBro staining; $n = 3$) and relative amounts of dimers are given at the bottom. RU, relative units. (B and C) HeLa cells were exposed to selenite at the indicated concentrations for 17 h and were then analyzed for VDAC oligomerization by assessment of EGS-based cross-linking (B) or immunocytochemical assessment of Cyto *c* release (C). Control and selenite-treated HeLa cells were stained with the mitochondrial marker MitoTracker red dye, followed by immunostaining with anti-cytochrome *c* antibodies and Alexa Fluor 488-conjugated secondary antibodies (green), and visualized by confocal microscopy. The arrow in panel B indicates an anti-VDAC1 antibody-labeled protein band migrating below the position of monomeric VDAC.

STS also induced VDAC oligomerization, in all cell types used. STS increased the levels of VDAC dimers, tetramers, and multimers in T-REx-293, HeLa, and T47D cells (Fig. 3A). The results of quantitative analysis of the extent of STS-induced apoptosis in the various cell types are shown in Fig. 3B.

When antibodies against Bax and Bak were used to verify the presence of Bax and/or Bak in the VDAC1-containing oligomers, no heterodimers or oligomers composed of VDAC and Bax or Bak were found. Similarly, it has been reported previously that Bax does not interact with either the VDAC or the adenine nucleotide transporter (ANT) in the mitochondria (31). Moreover, VDAC oligomerized regardless of the expression levels of proapoptotic proteins, e.g., Bax, Bak, and Bid, even in cells expressing undetectable levels of Bax, such as T-REx-293 or HeLa cells (Fig. 3C), suggesting that in these cells Bax is not a major component of the apoptotic machinery.

VDAC1 overexpression induces apoptotic cell death and VDAC oligomerization. Overexpression of human, murine, or rice VDAC1 was previously found to induce apoptotic cell death in all cell types tested (3, 19, 61). Here we found that overexpression of recombinant murine VDAC1 (mVDAC1), rat VDAC1 (rVDAC1), or mutated mVDAC1, such as E72Q-mVDAC1 or E202Q-mVDAC1, in T-REx cells resulted in cell death and VDAC oligomerization (Fig. 4). The levels of VDAC oligomers were greatly increased in VDAC1-overexpressing cells (Fig. 4A). Quantitative analysis of apoptotic cells, employing acridine orange and ethidium bromide staining (Fig. 4B), showed that about 55% of the cells had died ~105 h after transfection with plasmids encoding the various versions of VDAC1 (Fig. 4C). Thus, overexpression of VDAC1 from various sources resulted not only in apoptotic cell death but also in VDAC oligomerization.

VDAC oligomerization monitored in live cells using BRET2. Next, to explore the interactions between VDAC1 monomers and to directly monitor the oligomeric state of VDAC1 molecules in their native cellular membranes, we used bioluminescence resonance energy transfer (BRET2) technology (Fig. 5A) (4, 9). In BRET2 technology, VDAC1 proteins are tagged with either *Renilla* luciferase (RLuc) as the donor or a variant of GFP (GFP2) as the acceptor. Energy transfer occurs when the donor and acceptor are spatially close (<10 nm apart), making the technique ideal for monitoring protein-protein in-

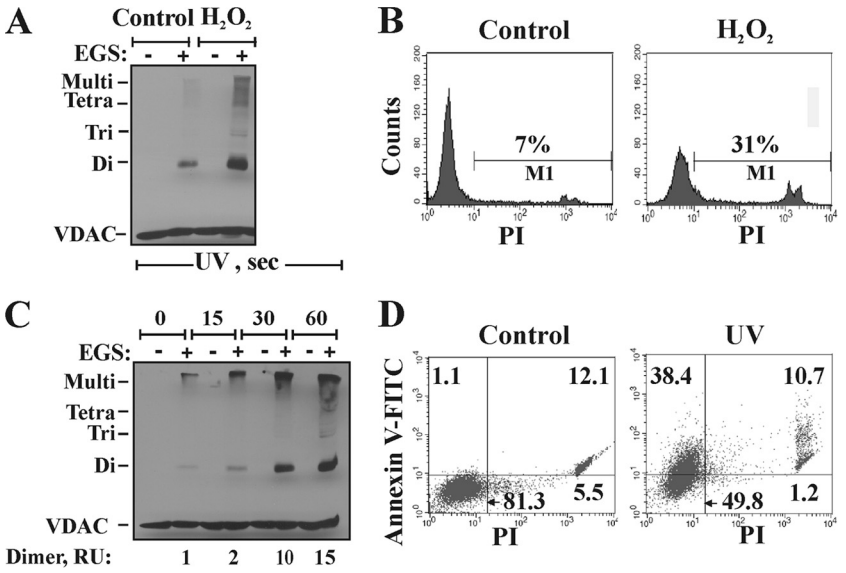

FIG. 2. H_2O_2- and UV-induced VDAC oligomerization. (A and B) T-REx-293 cells were incubated for 5 h with 1 mM H_2O_2, harvested, and subjected either to cross-linking with EGS (250 μM) as for Fig. 1 (A) or to apoptosis analysis via PI uptake and FACS analysis (B). The results of one experiment representative of three similar experiments are shown. (C) Cells were exposed to UV irradiation for the indicated times and were analyzed after 24 h for VDAC oligomerization by using EGS-based cross-linking and immunoblotting, as described for panel A. The relative amounts of dimers are given (RU, relative units), and the positions of VDAC monomers to tetramers and multimers are indicated. (D) Apoptosis, induced by UV irradiation, was assayed using annexin V–FITC–PI staining and FACS analysis. Results from one experiment representative of two similar experiments are shown.

teractions in biological systems (14). Enhancement of the BRET2 signal corresponds to activation of VDAC1 oligomerization, while attenuation of the apoptosis-enhanced BRET2 signal indicates inhibition of VDAC1 oligomerization.

DNAs encoding the genetically engineered fusion proteins rVDAC1–Rluc (in which RLuc was connected to rVDAC1 at the C-terminal position through a linker [GGGGS]) and rVDAC1–GFP2 (in which GFP2 was fused through the linker to the C terminus of rVDAC1) were cloned into BRET2 vectors. rVDAC1–GFP2 and rVDAC1–Rluc were expressed in T-REx cells stably expressing hVDAC1 shRNA, with a low level of endogenous hVDAC1 (2). The VDAC1 shRNA, being specific to human VDAC1, allowed the expression of rVDAC1 and decreased the participation of endogenous hVDAC in oligomerization, thereby enhancing the BRET2 signal. The expression levels of rVDAC1–GFP2 and rVDAC1–Rluc (Fig. 5C) were correlated with the amounts of plasmids used. For rVDAC1–GFP2 and rVDAC1–Rluc, 0.8 μg and 0.1 μg, respectively, were found to give the best signal.

The results in Fig. 5B show that the BRET2 technology is applicable for use with the well-defined apoptosis inducers STS, As_2O_3, and sodium selenite. All these apoptosis inducers

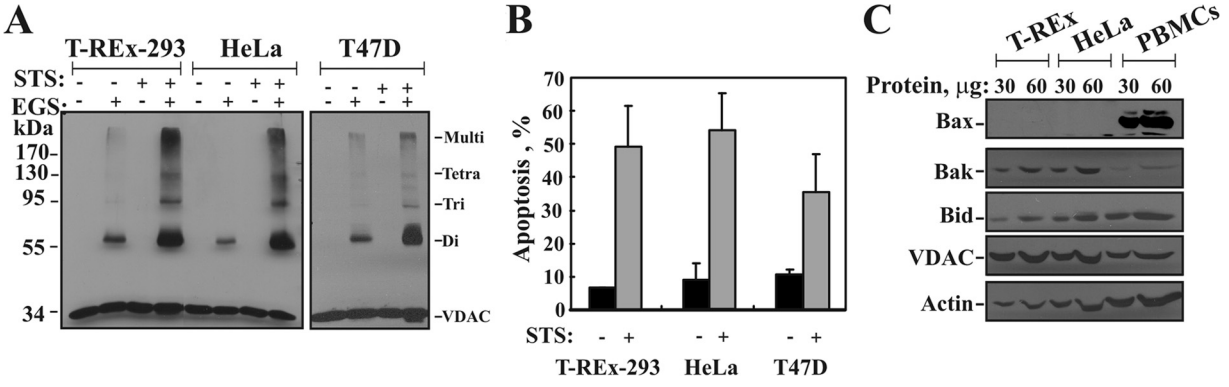

FIG. 3. STS induces VDAC oligomerization in all cell types used. (A) T-REx-293, HeLa, and T47D cells (2.5 mg/ml) were incubated in the absence or presence of STS (1.25 μM; 5 h) and were subjected to cross-linking with EGS (250 μM) and to immunoblotting using anti-VDAC antibodies. The positions of molecular size protein standards are provided. (B) Quantitative analysis of apoptosis (assayed via AcrOr-EthBro staining) (n = 3). (C) T-REx-293, HeLa, and human peripheral blood mononuclear cells (PBMCs; isolated using Ficoll-Paque density gradient centrifugation) (30 and 60 μg) were subjected to immunoblotting using anti-Bax, anti-Bak, anti-Bid, and anti-VDAC antibodies. As a loading control, actin levels in the samples were determined using antiactin antibodies. Note that the increase in the amount of protein loaded was seen for all immunoblotted proteins, except for VDAC, due to the high affinity of the antibodies used, which yielded a saturated signal over 30 μg.

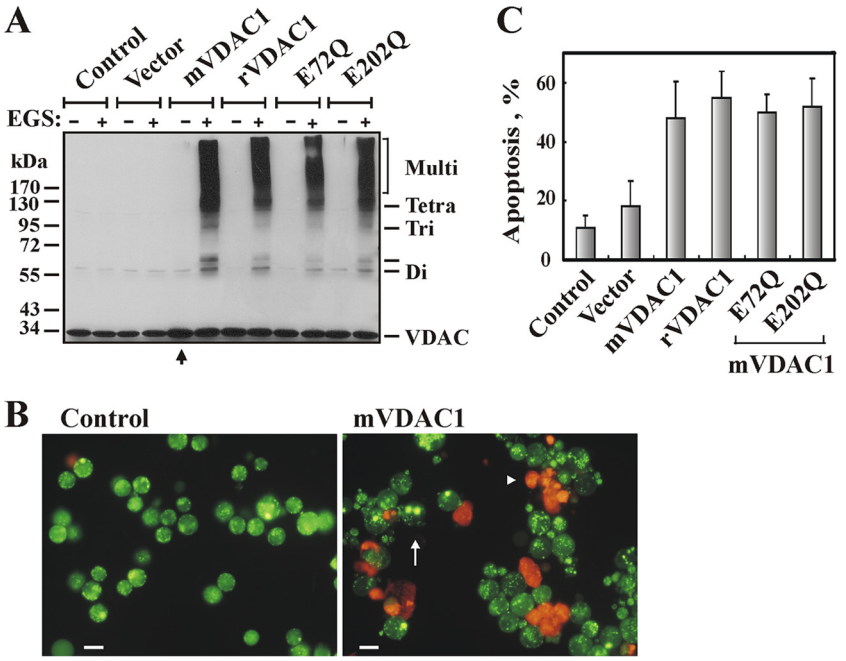

FIG. 4. VDAC1 overexpression induces VDAC oligomerization and apoptotic cell death. (A) T-REx-293 cells were transfected to overexpress murine VDAC1 (mVDAC1), rat VDAC1 (rVDAC1), E72Q-mVDAC1, or E202Q-mVDAC1. At 72 h following transfection, cells were incubated with EGS (75 μM) for 15 min and were then subjected to SDS-PAGE and immunoblotting. At the relatively low EGS concentration used, VDAC oligomers were obtained in cells overexpressing VDAC1 but not in nontransfected control cells. An additional band, above the dimer, appeared in cells overexpressing VDAC1 (indicated by a hyphen). (B) Apoptosis in cells overexpressing native or mutated VDAC1 was analyzed by use of AcrOr-EthBro staining 105 h following transfection. The arrow indicates cells in an early apoptotic state, reflected by degraded nuclei (stained green with acridine orange). The arrowhead indicates cells in the late apoptotic state (stained orange with acridine orange and ethidium bromide). Bars, 15 μm. (C) Quantitative analysis of apoptosis showed that at 105 h posttransfection, about 55% of the cells presented apoptotic characteristics.

enhanced the BRET2 signal (GFP2/RLuc ratio) in rVDAC1–Rluc- and rVDAC1–GFP2-expressing cells by 4- to 5-fold over that in cells not exposed to an apoptosis inducer (Fig. 5B). As expected, treatment with STS did not affect the BRET2 signal in control cells (data not shown).

DIDS, an apoptosis inhibitor, prevents VDAC oligomerization. To further demonstrate the relationship between apoptosis and VDAC oligomerization, we tested the effect of the apoptosis inhibitor DIDS on STS-induced VDAC oligomerization (Fig. 6). DIDS was previously shown to interact with VDAC1 (46) and to inhibit apoptosis induced by various stimuli (19, 38). Here we demonstrated that DIDS prevented both STS-induced VDAC oligomerization (Fig. 6A) and apoptosis (Fig. 6B and C).

We also used the BRET2-based oligomerization assay to demonstrate that inhibition of apoptosis was accompanied by prevention of VDAC1 oligomerization (Fig. 6D). The results clearly showed that while STS enhanced the BRET2 signal by about 4-fold, preincubation of the cells with DIDS prevented such STS-induced BRET2 signal enhancement. Thus, in contrast to apoptosis inducers, apoptosis inhibitors inhibited VDAC1 oligomerization, reinforcing the idea that the formation of VDAC1 oligomers is involved in apoptosis.

Relationship between the extent of apoptosis and the level of VDAC oligomerization. To further investigate the relationship between apoptosis induction and VDAC oligomerization, both processes were analyzed as a function of the concentration of the apoptosis inducer STS and as a function of the duration of incubation with H_2O_2 (Fig. 7). We found that the occurrence of both apoptosis and VDAC oligomerization increased upon the exposure of cells to various concentrations of STS (Fig. 7A and B). Quantitative analysis showed a linear relationship between changes in the amounts of VDAC dimers and trimers, as stabilized by EGS cross-linking and revealed by immunoblotting (Fig. 7A), and the extent of apoptotic cell death, as a function of STS concentration (Fig. 7B). Furthermore, the same time course for VDAC oligomerization (Fig. 7C), apoptosis (Fig. 7D), and Cyto *c* release (Fig. 7E) was obtained when these processes were induced by H_2O_2 (Fig. 7F), revealing the close relationship between these processes.

Inhibition of caspase activity had no effect on VDAC oligomerization. To determine whether caspase activity is required or involved in VDAC oligomerization, we induced apoptosis in HeLa and T-REx cells with As_2O_3 and tested the effects of the pancaspase inhibitor z-VAD-fmk on VDAC1 oligomerization and Cyto *c* release (Fig. 8A and B). VDAC oligomerization (Fig. 8A) and the release of Cyto *c* (Fig. 8B), induced by As_2O_3, were not significantly modified by the concentrations of z-VAD-fmk used. It should be noted, however, that in HeLa cells, but not in T-REx cells, z-VAD-fmk at 5 μM showed some inhibition of VDAC oligomerization but not of Cyto *c* release (Fig. 8A), with increased inhibition observed when high concentrations of the caspase inhibitor were applied (data not shown). This may result from a nonspecific effect of

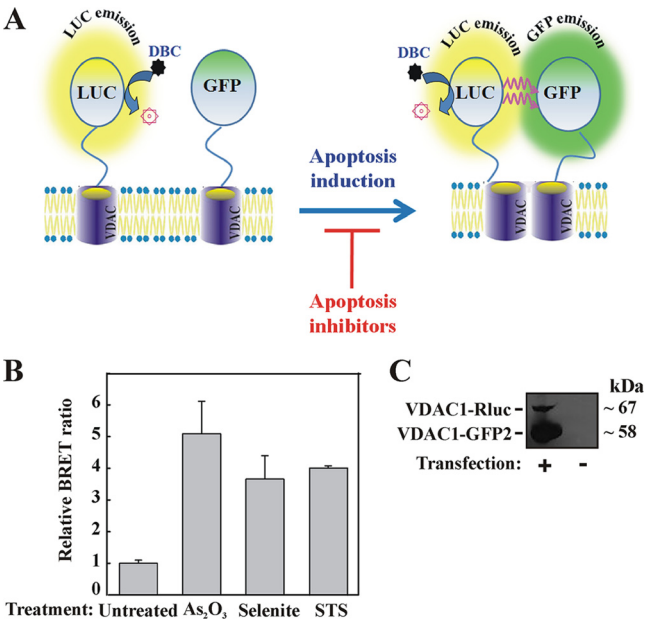

FIG. 5. VDAC1 oligomerization and BRET2-based assay. (A) Schematic representation showing energy transfer between VDAC1-luciferase (RLuc, a light-producing enzyme) as the donor and VDAC1-GFP2 (fluorophore) as the acceptor, which occurs only when the donor and the acceptor are spatially close. The BRET2 signal is obtained when the two VDAC1 molecules interact physically. Compounds enhancing apoptosis lead to VDAC1 oligomerization and thus enhance the BRET2 signal, while apoptosis inhibitors inhibit VDAC1 oligomerization and therefore decrease the BRET2 signal. The luciferase substrate DBC emits light upon cleavage and thus causes excitation of the proximal GFP2 protein, thereby generating the BRET2 signal. (B) STS, selenite, and As_2O_3 enhance the BRET2 signal. T-REx cells expressing hVDAC1 shRNA were cotransfected with plasmids encoding rVDAC1-Rluc (0.1 μg) and rVDAC1-GFP2 (0.8 μg). Luciferase and GFP signals were measured 72 h posttransfection. The BRET2 signals obtained in cells treated with STS (0.6 μM; 3 h), selenite (8 μM; 16 h), or As_2O_3 (20 μM; 16 h) are shown. "Untreated" refers to cells transfected with the rVDAC1-Rluc plasmid and treated with the appropriate amount of dimethyl sulfoxide. BRET2 signals were measured, and BRET2 ratios were calculated as described in Materials and Methods. The results were collected from three 96-well plates (STS) or one 96-well plate (selenite and As_2O_3). (C) Cellular expression levels of VDAC1-Rluc and VDAC1-GFP2, analyzed by immunoblotting using anti-VDAC1antibodies.

the inhibitor. As expected, at the concentrations used, z-VAD-fmk almost completely inhibited the activated caspases (Fig. 8C and D). The enzymatic activity of activated caspases was measured by the caspase cleavage of a luminogenic substrate containing the tetrapeptide sequence DEVD. z-VAD-fmk (2.5 or 5 μM) inhibited (by about 80%) the caspase activity activated by As_2O_3 (Fig. 8C), a result that was also reflected in the inhibition of PARP cleavage (Fig. 8D). These findings suggest that VDAC oligomerization precedes caspase activation and thus may precede Cyto *c* release, which leads to the activation of caspases.

DISCUSSION

Supramolecular organization of the VDAC and coupling of VDAC oligomerization to apoptosis. The involvement of the VDAC in Cyto *c* release and apoptosis has attracted interest on several fronts and has been the focus of many recent reviews (25, 27, 42, 44, 45). Several models have proposed that the VDAC (either alone or in conjunction with Bax/Bak) mediates the delivery of apoptotic proteins across the OMM, while there is substantial evidence for the formation of higher-order VDAC-containing complexes (1, 12, 21, 24, 44, 47, 48, 54, 62). Taking previous findings together with our present finding that VDAC oligomerization is enhanced in cultured cells upon apoptosis induction, we propose that VDAC oligomerization is involved in the release of Cyto *c* from mitochondria and the subsequent induction of apoptosis. In this study we provided experimental support for our proposal that dynamic VDAC oligomerization mediates the formation of a large, flexible pore between individual subunits of VDAC1, serving as a channel for Cyto *c* crossing the OMM (1, 44, 47, 62). We showed the following. (i) VDAC oligomerization can be enhanced severalfold upon induction of apoptosis, regardless of the cell type used. Various stimuli, such as STS, cisplatin, As_2O_3, curcumin, etoposide, selenite, TNF-α, H_2O_2, UV irradiation, or VDAC1 overexpression, all acting via different mechanisms, induced the formation of similar profiles of EGS-stabilized cross-linked VDAC dimers, trimers, tetramers, and higher-order VDAC1-containing complexes (Fig. 1 to 4). (ii) Induction of apoptotic cell death by VDAC1 overexpression, regardless of the VDAC1 source, enhanced VDAC oligomerization (Fig. 4). (iii) By use of BRET2 technology, apoptosis induction or inhibition and modulation of VDAC1 oligomerization were demonstrated in intact living cells (Fig. 5 and 6). (iv) The VDAC conductance (46) and apoptosis (19, 38) inhibitor DIDS also prevented VDAC oligomerization (Fig. 6). (v) A direct relationship between the extent of VDAC oligomerization and the extent of apoptosis was determined (Fig. 7). (vi) Moreover, a strong BRET2 signal was obtained with a donor-to-acceptor ratio of 1:8 (Fig. 5C), implying that VDAC complexes are composed of oligomers of the protein and not just of dimers. These findings clearly show that apoptosis induction is tightly coupled to VDAC oligomerization. Thus, we propose that apoptosis induction by various apoptogenic inducers or by VDAC1 overexpression shifts the dynamic VDAC equilibrium toward oligomerization, leading to the formation of a protein-conducting channel composed of homo-oligomers, allowing Cyto *c* release and subsequent apoptotic cell death (Fig. 9). Support for the involvement of VDAC oligomerization in apoptosis has also been presented in studies showing that the apoptosis-inducing effect of As_2O_3 could be attributed to the induction of VDAC homodimerization, which can be prevented by Bcl-x_L (65). In addition, cross-linking studies revealed that the hepatitis E virus ORF3 protein upregulated VDAC expression levels and enhanced levels of oligomeric VDAC (34).

Since VDAC1 overexpression resulted in enhanced oligomerization and apoptotic cell death (Fig. 4), it is possible that the enhancement of VDAC oligomerization caused by apoptosis inducers might result from the upregulation of the VDAC expression level. Indeed, it has been shown previously, using gene microarray techniques, that irradiation of apoptosis-sensitive cells, which typically induces apoptosis, caused strong VDAC upregulation (56), while a proteomics-based investigation of the anticancer effects of arbutin on A375 cells also found that the VDAC was upregulated (35). However, under

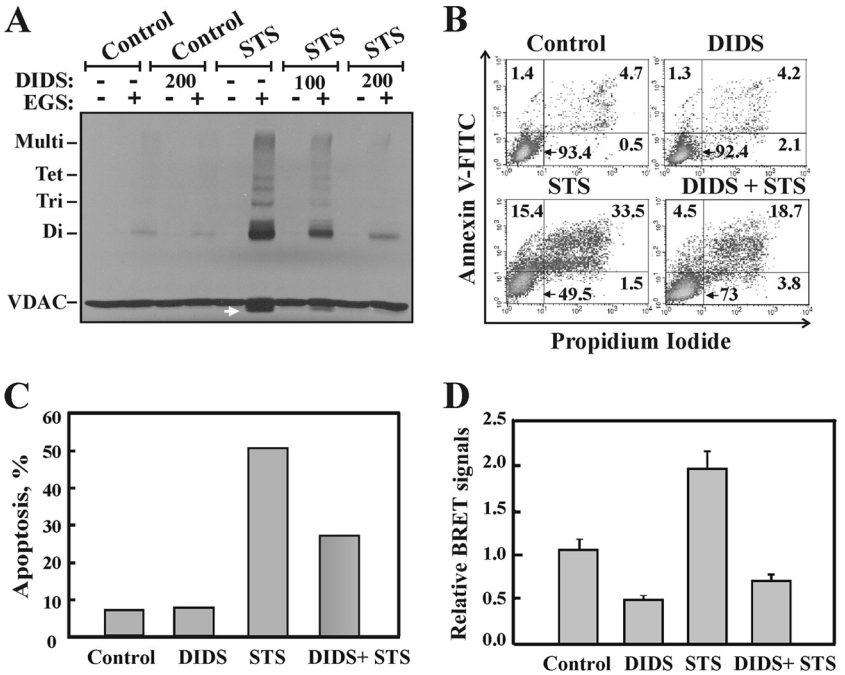

FIG. 6. DIDS inhibits VDAC oligomerization and apoptosis. (A) HeLa cells were incubated with DIDS (100 or 200 μM) for 1 h, after which they were incubated with or without STS (1.25 μM; 2 h), harvested, cross-linked with EGS (250 μM; 15 min), and then analyzed by immunoblotting using anti-VDAC antibodies. The dramatic inhibition of STS-induced VDAC oligomerization by DIDS is shown. (B) Representative FACS analysis of apoptotic cell death, assayed using annexin V–FITC–propidium iodide staining. (C) Quantitative analysis of apoptosis, as measured by FACS analysis (from panel B). Results of one experiment representative of three similar experiments are shown. (D) Ratios of the BRET2 signals obtained for cells treated with STS (0.8 μM; 3.0 h) with or without pretreatment with DIDS (100 μM; 1 h). T-REx-293 cells expressing VDAC1 shRNA were cotransfected with plasmids encoding rVDAC1–Rluc (0.1 μg) and rVDAC1–GFP2 (0.8 μg). Data are represented as means ± standard errors of the means.

the conditions used in this study to induce apoptosis, we observed no increase in VDAC expression levels as determined by Western blot analysis (data not shown).

Protein oligomerization as a mechanism for the mediation of Cyto *c* release and apoptosis. Oligomerization as a mechanism for the mediation of Cyto *c* release and apoptosis has also been proposed previously for two key proteins in the mitochondrial pathway of apoptosis, Bax and Bak (5, 6, 17, 30, 41, 43). Following apoptosis induction by STS or UV irradiation, monomeric Bax, either in the cytosol or weakly associated with mitochondria, became associated with mitochondria as a large oligomer/complex of 96 or 260 kDa (6, 17). These oligomeric forms of Bax, which were produced following the application of various apoptosis stimuli, were proposed to constitute the structural basis of the Cyto *c*-conducting channel in the OMM (5, 30, 50). In particular, apoptosis induction by TNF-α led to the activation of caspase-8, which cleaved Bid to tBid; this, in turn, led to the generation of Bax and Bak oligomers, forming complexes as large as 500 kDa (50). Our results showed that TNF-α also induced VDAC oligomerization (Fig. 1), hinting that a tBid-mediated process may also activate VDAC oligomerization. Additionally, cleaved Bid has been shown previously to modulate bilayer-reconstituted VDAC1 voltage gating (37), suggesting that tBid interacts directly with the VDAC.

The link between the multi-Bcl2 homology domain-containing, proapoptotic members Bax and/or Bak and VDAC oligomerization remains unclear. As_2O_3 induced the formation of Bax and VDAC hetero- and homo-oligomers, and Bax and the VDAC can form a large pore, which is permeable to Cyto *c* (41, 43). It has been suggested that both Bax and Bak interact physically with the VDAC (18). However, in our studies, we detected no hetero-oligomers comprising VDAC1 and Bax or Bak, and similarly, it has been reported previously that Bax does not interact with either the VDAC or the ANT in the mitochondria (31). It has also been reported that Cyto *c* release and apoptosis can take place in cells devoid of Bax (28, 33, 57, 58), and an extensive study suggested that Bax was not a major player in the functional loop causing the release of Cyto *c* (26). The expression level of Bax in the T-REx-293 and HeLa cells used in this study was undetectable, suggesting that in these cells, Bax is not a major component of the apoptosis machinery. Thus, we propose that VDAC1 homo-oligomers mediate an alternative route for Cyto *c* release. Nevertheless, although we detected no hetero-oligomers comprising VDAC1 and the proapoptotic protein Bax or Bak in our cell lines, we cannot rule out the possibility that such complexes exist in other cell lines.

The intraoligomer pore size for a VDAC oligomer is dependent on the number of VDAC monomers forming the pore. Based on our knowledge of the structure of VDAC monomers (12, 23, 54, 55), the association of six cylindrical VDAC1 monomers, each with an external diameter of 4.0 nm (representing the distance between the Cb of Phe236 and the Cb of Leu100), would result in a central pore with a diameter of 4 nm, thus forming a pathway large enough for the passage of Cyto *c*, which has a diameter of 3.4 nm (32) (Fig. 9). Further-

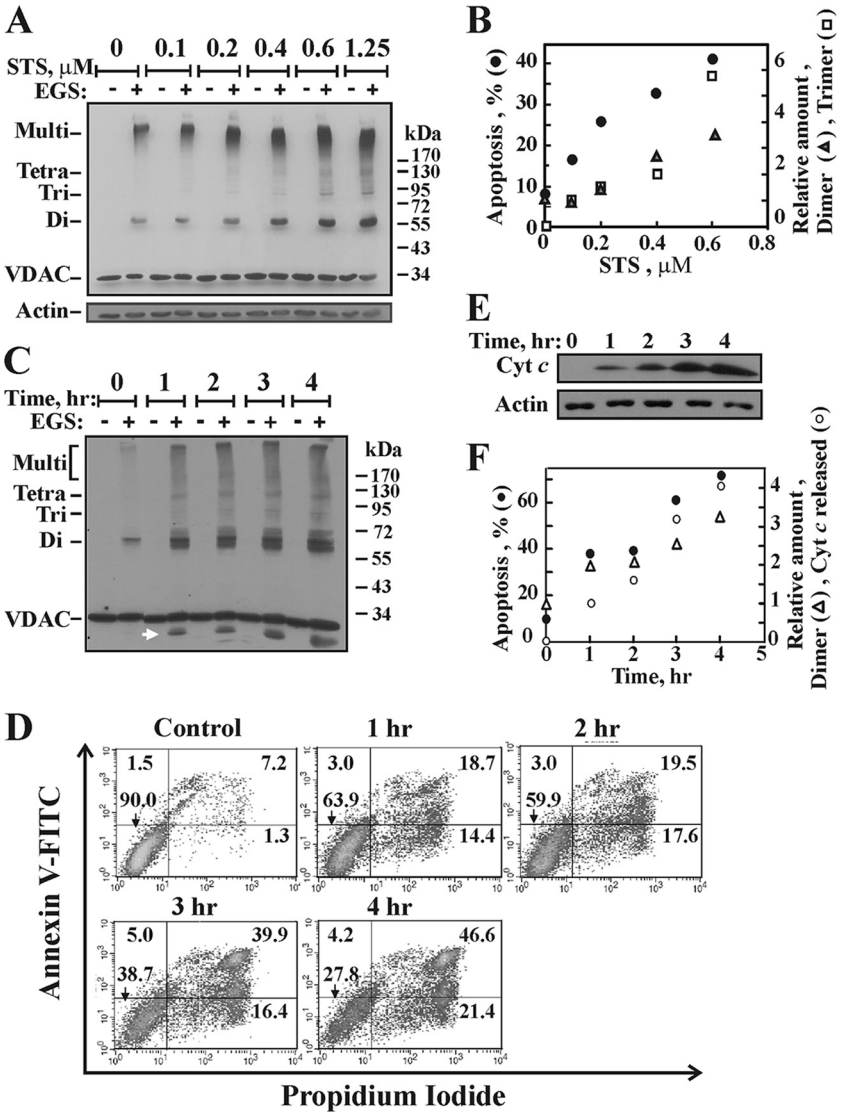

FIG. 7. Correlation between the extent of apoptosis and the level of VDAC oligomerization. (A) Immunoblot analysis shows the levels of VDAC oligomerization (cross-linking with 300 μM EGS for 15 min) induced by STS at various concentrations (0.1 to 0.6 μM for 16 h or 1.25 μM for 2.5 h) in T-REx-293 cells. (B) Quantitative analysis of the immunostained VDAC dimers and trimers and the extent of apoptosis, presented as a function of the STS concentration. (C to F) HeLa cells were exposed to H_2O_2 (12 mM) for the indicated times, after which VDAC oligomerization (C), apoptotic cell death (D), and Cyto *c* release (E) were analyzed and presented as a function of time (F).

more, if the VDAC1 oligomer is composed of more than six monomers and/or is a dynamic and flexible complex, the diameter of the internal oligomer pore may be even larger than 4 nm. This concept is similar to that previously described for the insertion of a Bax oligomer into the membrane to create a suitable pore for the release of Cyto *c* (5, 6, 17, 30, 41, 43).

VDAC1 oligomerization and signaling. It is well accepted that diverse apoptotic stimuli converge on a common apoptotic pathway leading to OMM permeabilization, resulting in the release to the cytosol of molecules (e.g., Cyto *c* and AIF) that are crucial for the activation of downstream effectors of apoptosis, i.e., caspases, leading to manifestations of apoptotic cell death. However, the events that take place before OMM permeabilization remain unclear. Our results point to VDAC1 oligomerization as a general mechanism common to numerous apoptogens acting via different initiating cascades.

To address the sequence of events related to VDAC1 oligomerization, we asked whether caspase activation is needed for VDAC oligomerization. It is well accepted that Cyto *c* release is initiated and completed several minutes before caspase-3/7 activity becomes detectable (26); thus, caspase-3 is activated downstream of Cyto *c* release. Here we showed that while the activation of caspases, triggered by As_2O_3, was completely inhibited by the broad-spectrum pancaspase inhibitor z-VAD-fmk (Fig. 8C and D), VDAC oligomerization and Cyto *c* release were not (Fig. 8A and B). These results suggest that not only Cyto *c* release, but also VDAC oligomerization, is independent of caspase activity. Therefore, VDAC oligomerization

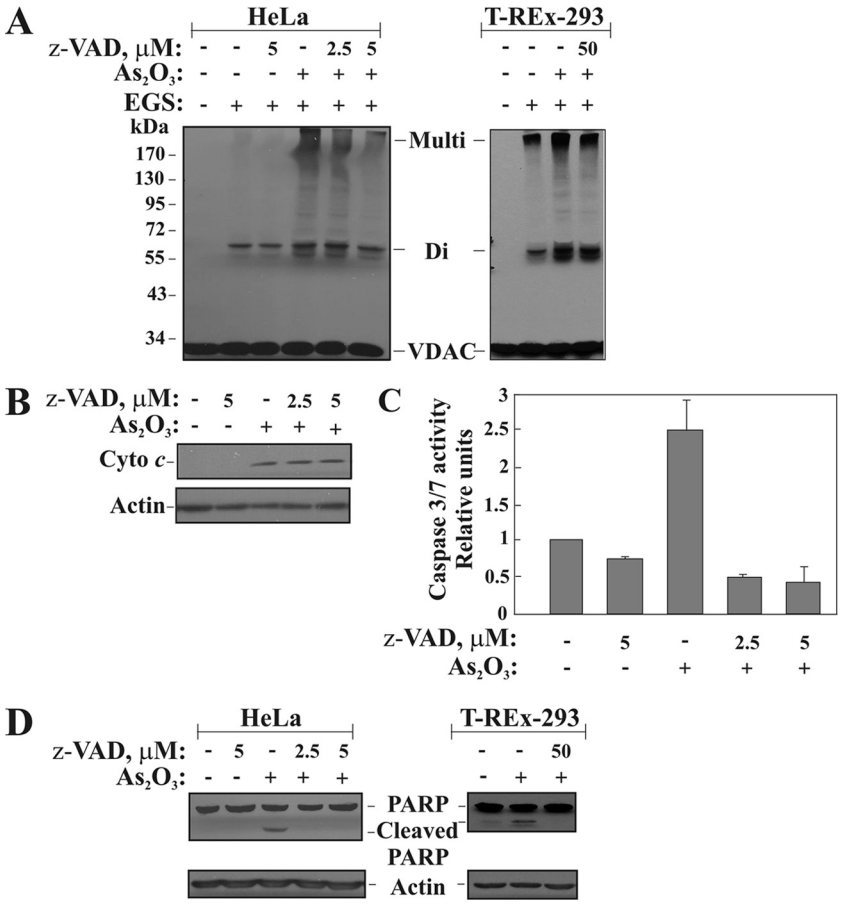

FIG. 8. Caspase activity is not required for VDAC oligomerization. Cells were preincubated with or without zVAD-fmk (2.5 or 5 μM with HeLa cells and 50 μM with T-REx cells, for 1.5 h), followed by As_2O_3 treatment (30 μM for 17 h). (A and B) Cells were analyzed for VDAC oligomerization (A) and Cyto *c* release (B). (C) The enzymatic activities of the caspases were followed by measuring the bioluminescent signals using a microplate reader, as described in Materials and Methods. (D) Caspase activity, as reflected by PARP cleavage, was analyzed by immunoblotting. The immunoblot was probed with a rabbit anti-PARP polyclonal antibody. Immunoblotting of actin, as a loading control, is also presented.

must precede the activation of caspases and may precede Cyto *c* release, which leads to caspase activation.

The various apoptosis activation signals found to induce VDAC oligomerization act upstream of Cyto *c* release. However, for any given apoptotic pathway, the molecular details of the upstream events leading to oligomerization, such as when the events induced by STS, curcumin, H_2O_2, As_2O_3, etoposide, cisplatin, selenite, or UV irradiation are transmitted to mitochondria, triggering VDAC1 oligomerization, are unknown. For example, STS, which is generally considered to mediate

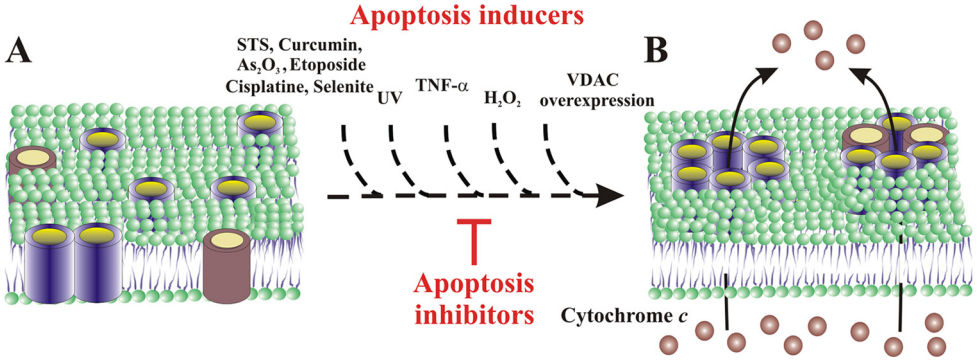

FIG. 9. Model for apoptotic signals inducing VDAC1 oligomerization-mediated Cyto *c* release. (A) Side view of membranal VDAC1 (in blue) and a proapoptotic protein (in red), both predominantly in the monomeric state. (B) When an apoptotic signal (e.g., STS, curcumin, As_2O_3, etoposide, cisplatin, selenite, TNF-α, H_2O_2, UV irradiation, or VDAC1 overexpression) is encountered, oligomerization of VDAC as homo- or hetero-oligomers is enhanced, leading to pore formation between VDAC β-barrel monomers. While apoptosis inducers facilitate homo- and/or hetero-oligomer formation, apoptosis inhibitors (e.g., DIDS) inhibit such oligomerization and thereby inhibit Cyto *c* release and apoptotic cell death.

apoptosis through a mitochondrion-mediated mechanism, is an inhibitor of protein kinase C and other protein kinases and induces apoptosis via various cellular events, including suppression of p38 phosphorylation and activation of Jun N-terminal protein kinase (JNK) (64). Curcumin-induced apoptosis has been shown to involve mainly a mitochondrion-mediated pathway in various cancer cells originating from different tissues (16). Cell death induced by As_2O_3 was found to coincide with Cyto *c* release, indicating activation through the mitochondrial apoptosis pathway (65). Apoptosis induction by cisplatin required p53-mediated activation of p38a mitogen-activated protein kinase (MAPK) through the generation of reactive oxygen species (ROS), with mitochondria being a critical target (59). Furthermore, cisplatin interacted directly with the VDAC (59), and cisplatin-induced Bax activation, Cyto *c* and AIF release, and caspase-3 maturation were reduced in cells in which VDAC1 expression was suppressed (51).

A factor that may contribute to the modulation of the VDAC's oligomeric state is its phosphorylation state. VDAC1 possesses a number of potential phosphorylatable residues, several of which have been shown to undergo phosphorylation (11, 13). Thus, it is possible that protein kinases control VDAC oligomerization by phosphorylating the VDAC itself or its binding partners. Direct modification of the oxidation state of the VDAC may also affect its oligomeric form. It has been suggested that Cyto *c* release is a ROS-dependent process (36). H_2O_2-induced apoptosis has been shown to be inhibited by DIDS or anti-VDAC antibodies (29). Moreover, it has been proposed that some anticancer agents induce caspase-dependent apoptosis in cancer cells by production of ROS via the quinone-reducing activity of VDAC1 (49). In our study, H_2O_2 induced VDAC oligomerization (Fig. 2), while DIDS inhibited it (Fig. 6). A previous study revealed that ROS may also affect VDAC oligomerization indirectly, by oxidation of cardiolipin and dissociation of Cyto *c* from this lipid (36). This, together with our finding that VDAC oligomerization is highly encouraged by Cyto *c* (62), suggests that unbound Cyto *c* promotes VDAC oligomerization, Cyto *c* release, and subsequent apoptosis.

Finally, VDAC overexpression resulted in a dramatic increase in the oligomeric status of the VDAC (Fig. 4) and in apoptotic cell death (2, 19, 44, 47, 61). Although the mechanism underlying the induction of cell death by VDAC1 overexpression remains unclear, our results suggest that this may be mediated via VDAC oligomerization, leading to enhanced activation of caspase-9 and elevated production of ROS (60). It should be noted that apoptosis induced by VDAC1 overexpression has common features with apoptosis induced by other stimuli (e.g., STS, H_2O_2), such as inhibition by RuR (61), Bcl2 (19), HK-I overexpression (3, 8, 61), or DIDS (19), all agents that interact with VDAC.

To conclude, the results presented here show that all apoptosis inducers, irrespective of their chemical formulae and mechanisms of action, induced VDAC oligomerization, indicating a strong coupling between VDAC oligomerization and apoptosis induction. Thus, VDAC oligomerization is likely a common denominator of mitochondrion-mediated apoptosis. Furthermore, VDAC oligomerization plays a crucial role in many apoptotic signaling cascades allowing the OMM to become permeable to Cyto *c*, thereby allowing the initiation of downstream apoptotic events. Thus, targeting of the oligomeric status of VDAC, and hence of apoptosis, offers a therapeutic strategy for combating cancers and neurodegenerative diseases.

ACKNOWLEDGMENT

This work was supported by a grant (647/09) from the Israel Science Foundation.

REFERENCES

1. **Abu-Hamad, S., N. Arbel, D. Calo, L. Arzoine, A. Israelson, N. Keinan, R. Ben-Romano, O. Friedman, and V. Shoshan-Barmatz.** 2009. The VDAC1 N-terminus is essential both for apoptosis and the protective effect of anti-apoptotic proteins. J. Cell Sci. **122:**1906–1916.
2. **Abu-Hamad, S., S. Sivan, and V. Shoshan-Barmatz.** 2006. The expression level of the voltage-dependent anion channel controls life and death of the cell. Proc. Natl. Acad. Sci. U. S. A. **103:**5787–5792.
3. **Abu-Hamad, S., H. Zaid, A. Israelson, E. Nahon, and V. Shoshan-Barmatz.** 2008. Hexokinase-I protection against apoptotic cell death is mediated via interaction with the voltage-dependent anion channel-1: mapping the site of binding. J. Biol. Chem. **19:**13482–13490.
4. **Angers, S., A. Salahpour, E. Joly, S. Hilairet, D. Chelsky, M. Dennis, and M. Bouvier.** 2000. Detection of β2-adrenergic receptor dimerization in living cells using bioluminescence resonance energy transfer (BRET). Proc. Natl. Acad. Sci. U. S. A. **97:**3684–3689.
5. **Annis, M. G., E. L. Soucie, P. J. Dlugosz, J. A. Cruz-Aguado, L. Z. Penn, B. Leber, and D. W. Andrews.** 2005. Bax forms multispanning monomers that oligomerize to permeabilize membranes during apoptosis. EMBO J. **24:** 2096–2103.
6. **Antonsson, B., S. Montessuit, B. Sanchez, and J. C. Martinou.** 2001. Bax is present as a high molecular weight oligomer/complex in the mitochondrial membrane of apoptotic cells. J. Biol. Chem. **276:**11615–11623.
7. **Arzoine, L., N. Zilberberg, R. Ben-Romano, and V. Shoshan-Barmatz.** 2009. Voltage-dependent anion channel 1-based peptides interact with hexokinase to prevent its anti-apoptotic activity. J. Biol. Chem. **284:**3946–3955.
8. **Azoulay-Zohar, H., A. Israelson, S. Abu-Hamad, and V. Shoshan-Barmatz.** 2004. In self-defence: hexokinase promotes voltage-dependent anion channel closure and prevents mitochondria-mediated apoptotic cell death. Biochem. J. **377:**347–355.
9. **Bacart, J., C. Corbel, R. Jockers, S. Bach, and C. Couturier.** 2008. The BRET technology and its application to screening assays. Biotechnol. J. **3:**311–324.
10. **Baines, C. P., R. A. Kaiser, T. Sheiko, W. J. Craigen, and J. D. Molkentin.** 2007. Voltage-dependent anion channels are dispensable for mitochondrial-dependent cell death. Nat. Cell Biol. **9:**550–555.
11. **Baines, C. P., C. X. Song, Y. T. Zheng, G. W. Wang, J. Zhang, O. L. Wang, Y. Guo, R. Bolli, E. M. Cardwell, and P. Ping.** 2003. Protein kinase ε interacts with and inhibits the permeability transition pore in cardiac mitochondria. Circ. Res. **92:**873–880.
12. **Bayrhuber, M., T. Meins, M. Habeck, S. Becker, K. Giller, S. Villinger, C. Vonrhein, C. Griesinger, M. Zweckstetter, and K. Zeth.** 2008. Structure of the human voltage-dependent anion channel. Proc. Natl. Acad. Sci. U. S. A. **105:**15370–15375.
13. **Bera, A. K., S. Ghosh, and S. Das.** 1995. Mitochondrial VDAC can be phosphorylated by cyclic AMP-dependent protein kinase. Biochem. Biophys. Res. Commun. **209:**213–217.
14. **Bertrand, L., S. Parent, M. Caron, M. Legault, E. Joly, S. Angers, M. Bouvier, M. Brown, B. Houle, and L. Menard.** 2002. The BRET2/arrestin assay in stable recombinant cells: a platform to screen for compounds that interact with G protein-coupled receptors (GPCRS). J. Recept. Signal Transduct. Res. **22:**533–541.
15. **Doran, E., and A. P. Halestrap.** 2000. Cytochrome *c* release from isolated rat liver mitochondria can occur independently of outer-membrane rupture: possible role of contact sites. Biochem. J. **348:**343–350.
16. **Duvoix, A., R. Blasius, S. Delhalle, M. Schnekenburger, F. Morceau, E. Henry, M. Dicato, and M. Diederich.** 2005. Chemopreventive and therapeutic effects of curcumin. Cancer Lett. **223:**181–190.
17. **Eskes, R., S. Desagher, B. Antonsson, and J. C. Martinou.** 2000. Bid induces the oligomerization and insertion of Bax into the outer mitochondrial membrane. Mol. Cell. Biol. **20:**929–935.
18. **Galluzzi, L., and G. Kroemer.** 2007. Mitochondrial apoptosis without VDAC. Nat. Cell Biol. **9:**487–489.
19. **Godbole, A., J. Varghese, A. Sarin, and M. K. Mathew.** 2003. VDAC is a conserved element of death pathways in plant and animal systems. Biochim. Biophys. Acta **1642:**87–96.
20. **Gogvadze, V., S. Orrenius, and B. Zhivotovsky.** 2006. Multiple pathways of cytochrome *c* release from mitochondria in apoptosis. Biochim. Biophys. Acta **1757:**639–647.
21. **Gonçalves, R. P., N. Buzhynskyy, V. Prima, J. N. Sturgis, and S. Scheuring.**

2007. Supramolecular assembly of VDAC in native mitochondrial outer membranes. J. Mol. Biol. **369:**413–418.
22. **Guo, X. W., P. R. Smith, B. Cognon, D. D'Arcangelis, E. Dolginova, and C. A. Mannella.** 1995. Molecular design of the voltage-dependent, anion-selective channel in the mitochondrial outer membrane. J. Struct. Biol. **114:**41–59.
23. **Hiller, S., R. G. Garces, T. J. Malia, V. Y. Orekhov, M. Colombini, and G. Wagner.** 2008. Solution structure of the integral human membrane protein VDAC-1 in detergent micelles. Science **321:**1206–1210.
24. **Hoogenboom, B. W., K. Suda, A. Engel, and D. Fotiadis.** 2007. The supramolecular assemblies of voltage-dependent anion channels in the native membrane. J. Mol. Biol. **370:**246–255.
25. **Kroemer, G., L. Galluzzi, and C. Brenner.** 2007. Mitochondrial membrane permeabilization in cell death. Physiol. Rev. **87:**99–163.
26. **Lartigue, L., C. Medina, L. Schembri, P. Chabert, M. Zanese, F. Tomasello, R. Dalibart, D. Thoraval, M. Crouzet, F. Ichas, and F. De Giorgi.** 2008. An intracellular wave of cytochrome *c* propagates and precedes Bax redistribution during apoptosis. J. Cell Sci. **121:**3515–3523.
27. **Lemasters, J. J., and E. Holmuhamedov.** 2006. Voltage-dependent anion channel (VDAC) as mitochondrial governator—thinking outside the box. Biochim. Biophys. Acta **1762:**181–190.
28. **Lindenboim, L., S. Kringel, T. Braun, C. Borner, and R. Stein.** 2005. Bak but not Bax is essential for Bcl-xS-induced apoptosis. Cell Death Differ. **12:**713–723.
29. **Madesh, M., and G. Hajnoczky.** 2001. VDAC-dependent permeabilization of the outer mitochondrial membrane by superoxide induces rapid and massive cytochrome *c* release. J. Cell Biol. **155:**1003–1015.
30. **Mikhailov, V., M. Mikhailova, K. Degenhardt, M. A. Venkatachalam, E. White, and P. Saikumar.** 2003. Association of Bax and Bak homo-oligomers in mitochondria. Bax requirement for Bak reorganization and cytochrome *c* release. J. Biol. Chem. **278:**5367–5376.
31. **Mikhailov, V., M. Mikhailova, D. J. Pulkrabek, Z. Dong, M. A. Venkatachalam, and P. Saikumar.** 2001. Bcl-2 prevents Bax oligomerization in the mitochondrial outer membrane. J. Biol. Chem. **276:**18361–18374.
32. **Mirkin, N., J. Jaconcic, V. Stojanoff, and A. Moreno.** 2008. High resolution X-ray crystallographic structure of bovine heart cytochrome *c* and its application to the design of an electron transfer biosensor. Proteins **70:**83–92.
33. **Mizuta, T., S. Shimizu, Y. Matsuoka, T. Nakagawa, and Y. Tsujimoto.** 2007. A Bax/Bak-independent mechanism of cytochrome *c* release. J. Biol. Chem. **282:**16623–16630.
34. **Moin, S. M., M. Panteva, and S. Jameel.** 2007. The hepatitis E virus Orf3 protein protects cells from mitochondrial depolarization and death. J. Biol. Chem. **282:**21124–21133.
35. **Nawarak, J., R. Huang-Liu, S. H. Kao, H. H. Liao, S. Sinchaikul, S. T. Chen, and S. L. Cheng.** 2009. Proteomics analysis of A375 human malignant melanoma cells in response to arbutin treatment. Biochim. Biophys. Acta **1794:**159–167.
36. **Ott, M., J. D. Robertson, V. Gogvadze, B. Zhivotovsky, and S. Orrenius.** 2002. Cytochrome *c* release from mitochondria proceeds by a two-step process. Proc. Natl. Acad. Sci. U. S. A. **99:**1259–1263.
37. **Rostovtseva, T. K., B. Antonsson, M. Suzuki, R. J. Youle, M. Colombini, and S. M. Bezrukov.** 2004. Bid, but not Bax, regulates VDAC channels. J. Biol. Chem. **279:**13575–13583.
38. **Sade, H., N. S. Khandre, M. K. Mathew, and A. Sarin.** 2004. The mitochondrial phase of the glucocorticoid-induced apoptotic response in thymocytes comprises sequential activation of adenine nucleotide transporter (ANT)-independent and ANT-dependent events. Eur. J. Immunol. **34:**119–125.
39. **Shi, Y., J. Chen, C. Weng, R. Chen, Y. Zheng, Q. Chen, and H. Tang.** 2003. Identification of the protein-protein contact site and interaction mode of human VDAC1 with Bcl-2 family proteins. Biochem. Biophys. Res. Commun. **305:**989–996.
40. **Shilo, S., A. Aronis, R. Komarnitsky, and O. Tirosh.** 2003. Selenite sensitizes mitochondrial permeability transition pore opening in vitro and in vivo: a possible mechanism for chemo-protection. Biochem. J. **370:**283–290.
41. **Shimizu, S., T. Ide, T. Yanagida, and Y. Tsujimoto.** 2000. Electrophysiological study of a novel large pore formed by Bax and the voltage-dependent anion channel that is permeable to cytochrome *c*. J. Biol. Chem. **275:**12321–12325.
42. **Shimizu, S., Y. Matsuoka, Y. Shinohara, Y. Yoneda, and Y. Tsujimoto.** 2001. Essential role of voltage-dependent anion channel in various forms of apoptosis in mammalian cells. J. Cell Biol. **152:**237–250.
43. **Shimizu, S., M. Narita, and Y. Tsujimoto.** 1999. Bcl-2 family proteins regulate the release of apoptogenic cytochrome *c* by the mitochondrial channel VDAC. Nature **399:**483–487.
44. **Shoshan-Barmatz, V., N. Arbel, and L. Arzoine.** 2008. VDAC, the voltage-dependent anion channel: function, regulation and mitochondrial signaling in cell life and death. Cell Sci. **4:**74–118.
45. **Shoshan-Barmatz, V., V. De Pinto, M. Zweckstetter, Z. Raviv, N. Keinan, and N. Arbel.** 2010. VDAC, a multi-functional mitochondrial protein regulating cell life and death. Mol. Aspects Med. **31:**227–285.
46. **Shoshan-Barmatz, V., N. Hadad, W. Feng, I. Shafir, I. Orr, M. Varsanyi, and L. M. Heilmeyer.** 1996. VDAC/porin is present in sarcoplasmic reticulum from skeletal muscle. FEBS Lett. **386:**205–210.
47. **Shoshan-Barmatz, V., A. Israelson, D. Brdiczka, and S. Sheu.** 2006. The voltage-dependent anion channel (VDAC): function in intracellular signalling, cell life and cell death. Curr. Pharm. Des. **12:**2249–2270.
48. **Shoshan-Barmatz, V., R. Zalk, D. Gincel, and N. Vardi.** 2004. Subcellular localization of VDAC in mitochondria and ER in the cerebellum. Biochim. Biophys. Acta **1657:**105–114.
49. **Simamura, E., H. Shimada, T. Hatta, and K. Hirai.** 2008. Mitochondrial voltage-dependent anion channels (VDACs) as novel pharmacological targets for anti-cancer agents. J. Bioenerg. Biomembr. **40:**213–217.
50. **Sundararajan, R., A. Cuconati, D. Nelson, and E. White.** 2001. Tumor necrosis factor-alpha induces Bax-Bak interaction and apoptosis, which is inhibited by adenovirus E1B 19K. J. Biol. Chem. **276:**45120–45127.
51. **Tajeddine, N., L. Galluzzi, O. Kepp, E. Hangen, E. Morselli, L. Senovilla, N. Araujo, G. Pinna, N. Larochette, N. Zamzami, N. Modjtahedi, A. Harel-Bellan, and G. Kroemer.** 2008. Hierarchical involvement of Bak, VDAC1 and Bax in cisplatin-induced cell death. Oncogene **27:**4221–4232.
52. **Tomasello, F., A. Messina, L. Lartigue, L. Schembri, C. Medina, S. Reina, D. Thoraval, M. Crouzet, F. Ichas, V. De Pinto, and F. De Giorgi.** 2009. Outer membrane VDAC1 controls permeability transition of the inner mitochondrial membrane in cellulo during stress-induced apoptosis. Cell Res. **19:**1363–1376.
53. **Tsujimoto, Y., and S. Shimizu.** 2000. VDAC regulation by the Bcl-2 family of proteins. Cell Death Differ. **7:**1174–1181.
54. **Ujwal, R., D. Cascio, V. Chaptal, P. Ping, and J. Abramson.** 2009. Crystal packing analysis of murine VDAC1 crystals in a lipidic environment reveals novel insights on oligomerization and orientation. Channels (Austin) **3:**167–170.
55. **Ujwal, R., D. Cascio, J. P. Colletier, S. Faham, J. Zhang, L. Toro, P. Ping, and J. Abramson.** 2008. The crystal structure of mouse VDAC1 at 2.3 Å resolution reveals mechanistic insights into metabolite gating. Proc. Natl. Acad. Sci. U. S. A. **105:**17742–17747.
56. **Voehringer, D. W., D. L. Hirschberg, J. Xiao, Q. Lu, M. Roederer, C. B. Lock, L. A. Herzenberg, and L. Steinman.** 2000. Gene microarray identification of redox and mitochondrial elements that control resistance or sensitivity to apoptosis. Proc. Natl. Acad. Sci. U. S. A. **97:**2680–2685.
57. **Wan, K. F., S. L. Chan, S. K. Sukumaran, M. C. Lee, and V. C. Yu.** 2008. Chelerythrine induces apoptosis through a Bax/Bak-independent mitochondrial mechanism. J. Biol. Chem. **283:**8423–8433.
58. **Wei, M. C., W. X. Zong, E. H. Cheng, T. Lindsten, V. Panoutsakopoulou, A. J. Ross, K. A. Roth, G. R. MacGregor, C. B. Thompson, and S. J. Korsmeyer.** 2001. Proapoptotic BAX and BAK: a requisite gateway to mitochondrial dysfunction and death. Science **292:**727–730.
59. **Yang, Z., L. M. Schumaker, M. J. Egorin, E. G. Zuhowski, Z. Guo, and K. J. Cullen.** 2006. Cisplatin preferentially binds mitochondrial DNA and voltage-dependent anion channel protein in the mitochondrial membrane of head and neck squamous cell carcinoma: possible role in apoptosis. Clin. Cancer Res. **12:**5817–5825.
60. **Yuan, S., Y. Fu, X. Wang, H. Shi, Y. Huang, X. Song, L. Li, N. Song, and Y. Luo.** 2008. Voltage-dependent anion channel 1 is involved in endostatin-induced endothelial cell apoptosis. FASEB J. **22:**2809–2820.
61. **Zaid, H., S. Abu-Hamad, A. Israelson, I. Nathan, and V. Shoshan-Barmatz.** 2005. The voltage-dependent anion channel-1 modulates apoptotic cell death. Cell Death Differ. **12:**751–760.
62. **Zalk, R., A. Israelson, E. Garty, H. Azoulay-Zohar, and V. Shoshan-Barmatz.** 2005. Oligomeric states of the voltage-dependent anion channel and cytochrome *c* release from mitochondria. Biochem. J. **386:**73–83.
63. **Zeth, K., T. Meins, and C. Vonrhein.** 2008. Approaching the structure of human VDAC1, a key molecule in mitochondrial cross-talk. J. Bioenerg. Biomembr. **40:**127–132.
64. **Zhang, H., M. Vollmer, M. De Geyter, M. Durrenberger, and C. De Geyter.** 2005. Apoptosis and differentiation induced by staurosporine in granulosa tumor cells is coupled with activation of JNK and suppression of p38 MAPK. Int. J. Oncol. **26:**1575–1580.
65. **Zheng, Y., Y. Shi, C. Tian, C. Jiang, H. Jin, J. Chen, A. Almasan, H. Tang, and Q. Chen.** 2004. Essential role of the voltage-dependent anion channel (VDAC) in mitochondrial permeability transition pore opening and cytochrome *c* release induced by arsenic trioxide. Oncogene **23:**1239–1247.